

REPORT/PAPER, THESIS, or DISSERTATION

as a partial requirement
for
the course on

LASER METROLOGY AND NON-DESTRUCTIVE TESTING
ME 5304, C-2025

Finding the Wolf Tone: Acoustic analysis of violincello resonance properties using scanning laser Doppler vibrometry and holographic interferometry

Submitted by:



Stella Burfeind



Rupin Pradeep

Submitted to:

Professor Cosme Furlong-Vazquez

NEST – NanoEngineering, Science, and Technology
CHSLT- Center for Holographic Studies and Laser micro-mechatronics
Mechanical Engineering Department
School of Engineering
Worcester Polytechnic Institute
Worcester, MA 01609-2280

March 7th, 2025

Summary

This project aimed to perform acoustic analysis on the resonant properties of the violoncello, with the specific goal of detecting, isolating, and counteracting an auditory phenomenon known as the wolf tone. Cello performers typically place a tuned mass damper on the string affected by the wolf tone at a location correlated to the main resonant frequency of the cello body effectively to eliminate the tone from the cello. The resonant frequency of the cello body is first determined using scanning laser doppler vibrometry in the low frequency range where the wolf tone is typically found. Then holographic interferometry is used on the bridge to monitor effects of the tuned mass damper on resonance of the cello bridge, the part responsible for translating string vibration to the cello body. After placing the damper, scanning laser doppler vibrometry results remained unchanged and holographic interferometry showed removal of bridge resonance frequencies near the main body resonance, both of which were expected. In addition, playing the note where the wolf tone manifests proved that the wolf tone was no longer present. Therefore, it can be concluded that the wolf tone manifestation can be eliminated through nondestructive laser metrology techniques on the cello. However, further research can be done for more quantitative results including acoustic analysis and experimentation with damper placement rather than using a single calculated spot.

Acknowledgements

We would like to thank Prof. Furlong-Vazquez of the WPI Center for Holographic Studies and Laser micro-mechaTronics, as well as the PhD students of the CHSLT – Danny Ruiz-Cadalso, Howard Zheng, Anthony Salerni, and Jonathan Oliveira-Luiz – for their support and assistance with this project, and allowing us access to the lab and its equipment.

We would like to particularly thank Danny Ruiz-Cadalso for his time and effort troubleshooting the Holographic Interferometry setup and providing his MATLAB unwrapping code.

Table of Contents

Summary	2
Acknowledgements	3
List of Figures	5
List of Tables	5
1. Introduction	6
1.1 Wolf Tone Background	6
1.2 Scanning LDV Background	8
1.3 Time-Averaged Holographic Interferometry Basics	9
2. Methodology	10
2.1 Scanning LDV	10
2.2 Damper Placement	12
2.3 Time-Averaged Holographic Interferometry	13
2.4 Rerun Measurements	15
3. Results and Discussion	15
3.1 SLDV Results	15
3.2 Damper Placement	17
3.3 TAHII Results	18
4. Conclusions and Recommendations	19
References	21

List of Figures

1.1	Vibration of a string and cello body over time	7
1.2	Non-integer mode example antinode and node positions	8
2.1	Experimental test setup used for SLDV	10
2.2	Polytec PSV Acquisition mesh generation window	11
2.3	Experimental test setup used for holographic interferometry	14
2.4	Resultant signal image generated by the interferometer	14
2.5	MATLAB window displaying raw unwrapped data and filtered data	14
2.6	MATLAB interface to pick a “zero” point for the unwrapping algorithm	15
2.7	Generated displacement map upon conclusion of the program	15
3.1	Magnitude vs Frequency spectrum of undamped cello front plate	17
3.2	Magnitude vs Frequency spectrum of damped cello front plate	17
3.3	Damper mass and position from bridge plotted as a function of ability to reproduce the wolf tone after placing the damper	18

List of Tables

3.1	Resonance frequencies of the cello front body	16
3.2	Resonance frequencies of the cello bridge	19

1. Introduction

The wolf tone is a commonly found phenomenon of quality bowed string instruments. The distinctive and uncontrollable warbling or howling sound played at certain frequencies give the wolf tone its name. Most violoncello players choose to either play around this frequency or attempt to eliminate the tone with a correctly positioned tuned mass damper. This paper will present the use of scanning laser Doppler vibrometry (LDV) and time-averaged holographic interferometry (TAHI) in accurately finding the positioning of a tuned mass damper to eliminate the wolf tone of a given cello. The cello being examined is property of Stella Burfeind, a member of the research team.

There has not been much research conducted on wolf tone responses of stringed instruments. Notably, Vincent Debut, et. al. correlated tuned mass damper placement and weight to wolf tone reproducibility on a cello through single-point LDV and accelerometer readings of the affected string [3]. Additionally, Ailin Zhang, Jim Woodhouse, and George Stoppani conducted further research on the wolf tone through accelerometer readings of the cello bridge [4]. This paper builds upon these results through holographic interferometry scans of the bridge and definitive wolf tone measurements using scanning LDV.

1.1 Wolf Tone Background

The wolf tone appears when playing a string at a resonant frequency of the cello body. According to a study by C. V. Raman, playing at the body resonant frequency causes the body to dissipate the string vibrational energy at a rate greater than the bow can maintain the string position [2]. After losing energy, the damped string can no longer support the oscillations of

the cello body. Once the vibrations of the body lessen, the string can be supported by the bow again causing the damping cycle to repeat [2].

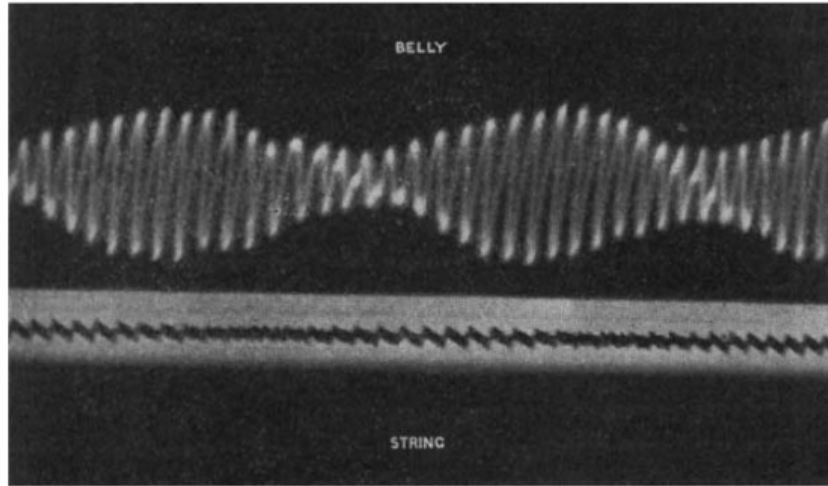


Fig. 1.1: Vibration of a string (top) and cello body (bottom) over time, showing the intermittent resonances [2]

The oscillation of undamped and damped vibrations creates the warbling or howling sound of the wolf tone as well as the uncontrollable characteristic of the string (Fig. 1). A resonance threshold for dissipating energy also indicates the possibility of many wolf tones depending on the manufacturing of the cello.

A tuned mass damper acts to prevent the wolf tone by drawing vibrational energy to itself. In contrast to the rate of energy drawn by the body, the energy drawn by the wolf damper allows the bow to maintain control of the string and continue playing a steady note. Since the tuned mass damper reduces vibrations, it's best to place the damper on an antinode of the wolf tone frequency to prevent other frequencies from being affected (Fig. 2). Other methods of dampening include strictly preventing body vibrations such as placing a tuned mass damper on the cello body or simply squeezing the body tightly with the legs while playing near the wolf tone frequency.

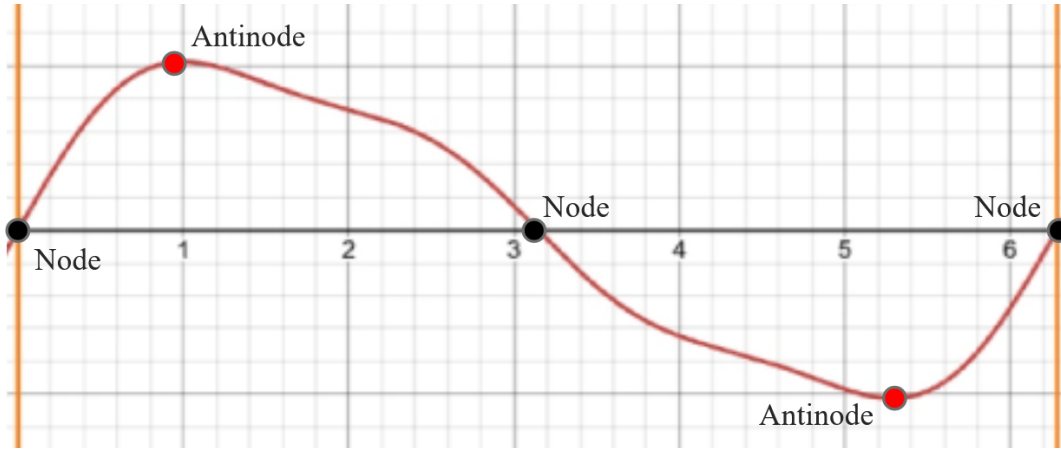


Fig. 1.2: Non-integer mode example antinode and node positions

1.2 Scanning LDV Background

Laser Doppler vibrometry provides velocity information at a point of reflection based on the Doppler effect. Integration and derivation of velocity over time gives displacement and acceleration values. Scanning LDV scans several points over a long period of time for full field velocity measurements.

A full SLDV system consists of a beam splitter, Bragg cell, photodetector, and other components to redirect light to the photodetector. The beam splitter creates two identical beams of frequency f_o . The first beam acts as a reference and is immediately redirected to the photodetector by a mirror. The second beam, object beam, is first reflected into a Bragg cell to shift the frequency by f_b , typically 40 MHz. Since the photodetector only detects phase difference, the positive shift f_b away from f_o allows for directional analysis. Without the Bragg cell, voltage characteristics of movement towards the camera would appear identical to similar movement away from the camera. For experiments with excitation frequency greater than 40 MHz, a different Bragg cell with higher f_b must be used.

After going through the Bragg cell, the laser is directed to the object. The Doppler effect adds a third frequency to the object beam upon reflection, f_d . The reflected light is redirected to the photodetector where the frequency difference between the object beam and reference beam is converted into voltage for measurement. From frequency difference, f_d can give velocity information by Eq. 1.1.

$$f_d = 2v(t) \frac{\cos(a)}{\lambda} \quad (1.1)$$

1.3 Time-Averaged Holographic Interferometry Basics

Holographic interferometry gives full view displacement characteristics. Laser light is split into a reference beam and object beam by a beam splitter. The reference beam is redirected to a photodetector and the object beam is directed to the object to be measured. Differences in distance cause an optical path difference between the object beam and reference beam. This results in fringe patterns recorded by the photodetector of varying displacement.

Time-averaged holographic interferometry takes advantage of the long exposure time for a hologram capture compared to one period of vibration cycle. Therefore, a single hologram is essentially a combination of several object positions in the vibration cycle with points of zero velocity contributing most to the image [1]. With a speaker excited sample, time-averaged holography clearly shows vibration patterns since points with zero velocity correspond to maximums and minimums.

Fringe patterns recorded by the photodetector can then be translated to displacement using Eq 1.2 where A is displacement, Δx is fringe distance, and λ is laser wavelength.

$$\Delta x = \frac{\lambda}{2A} \quad (1.2)$$

2. Methodology

2.1 Scanning LDV

Scanning LDV is required first to attain the resonant frequencies of the cello body. A two leg stand with three points of contact, one on the back and two on either side of the bottom, holds the cello on a vibration isolated table. Scanning LDV results are obtained using a PSV-500 scanning laser Doppler vibrometer from Polytec along with Polytec software. Since the stand tilts the cello body upwards seen in figure 1, the PSV-500 head is raised upwards and tilted down using a tripod. This is to reduce the magnitude of $\cos(\alpha)$ in Equation 1. A speaker with an amplifier is placed directly facing the cello aligned to the center of the body.

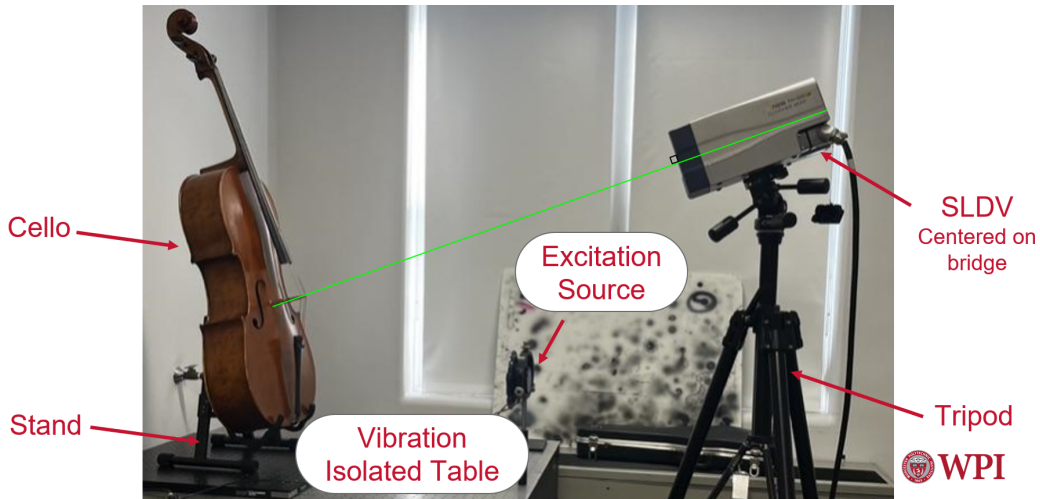


Fig 2.1: The experimental test setup used for SLDV

Running the scanning LDV and speaker excitation can be done entirely through Polytec hardware and software. Opening PSV Acquisition software, the first step is focusing the laser on the cello body using 2D alignment. Since the cello surface is not flat, several arbitrary contour points must be focused as seen in Figure 2. After focusing the laser, the measurement field is set.

To optimize the number of interior points with time cost, irregular mesh is used with density 30.

Areas separate from the cello body are cut out such as the neck, tailpiece, bridge, and f-holes.

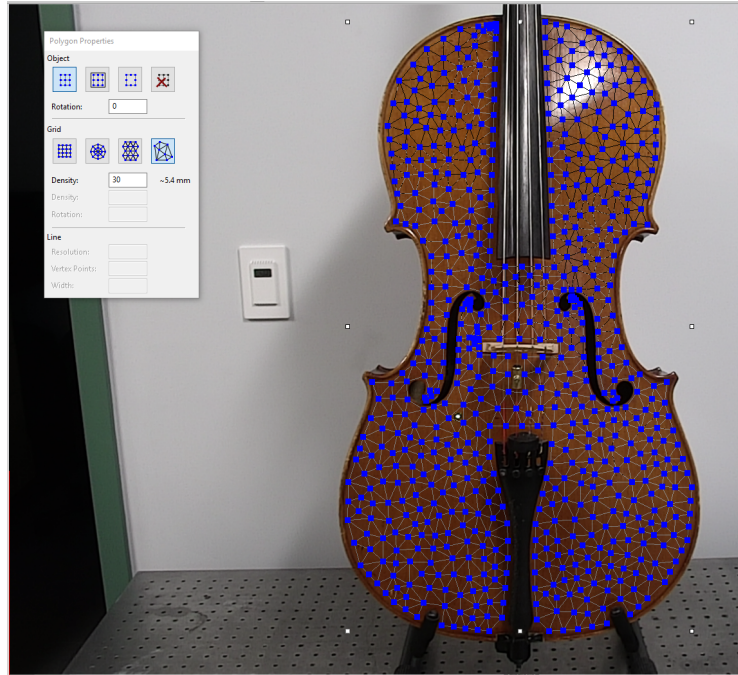


Fig 2.2: The Polytec PSV Acquisition mesh generation window

The Fast Fourier Transform scan settings are set to 0 - 400 Hz since wolf tone resonance frequencies are typically found between 100 and 300 Hz. 1600 frequency divisions allow for high frequency resolution and three complex averaging reduces effects of external noise. The default velocity threshold of 5 mm/s is sufficient for a 1V speaker amplification. However, the scan will automatically rerun points at a higher threshold if the velocity is greater than 5 mm/s. After running the scan, the results are viewed in PSV Analyzer. The view is changed from velocity to displacement as resonance is characterized by high magnitude vibrations. Then the highest peak around 185 Hz is the cello body main resonance. The frequency of the peak can be used for damper placement.

2.2 Damper Placement

The optimal tuned mass damper placement would be on the maximum displacement of the string at critical frequency, or essentially, an antinode of the critical frequency. Using the results of scanning LDV, the critical frequency is defined as the cello main body resonance. In order to find an antinode, the mode must first be calculated. If the string first harmonic frequency is known, the mode can be calculated using Eq 2.1 where f_1 is the first harmonic frequency and f_n is the critical frequency.

$$n = \frac{f_n}{f_1} \quad (2.1)$$

If the first harmonic frequency is unknown, it can be calculated using Eq 2.2 with characteristics of the string. Tension, T , and linear mass density, μ , would most likely have to be provided by the manufacturer. Length, L , may be provided or measured.

$$f_1 = \frac{1}{2} L \sqrt{\frac{T}{\mu}} \quad (2.2)$$

The string antinode positions can be found graphically using the superposition of integer modes with varying amplitudes to match the critical frequency mode as seen in Eq. 2.3.

$$n = \sum_{i=1}^j (x_i \cdot i) \quad (2.3)$$

Since n is typically between 1 and 2, values of i greater than 3 are considered negligible and the summation can be shortened to Eq. 2.4. Value A can be reduced to 1 by dividing each amplitude by A creating new amplitudes B' and C' seen in Equation 7.

$$n = A + 2B + 3C \quad (2.4)$$

$$n - 1 = 2B' + 3C' \quad (2.5)$$

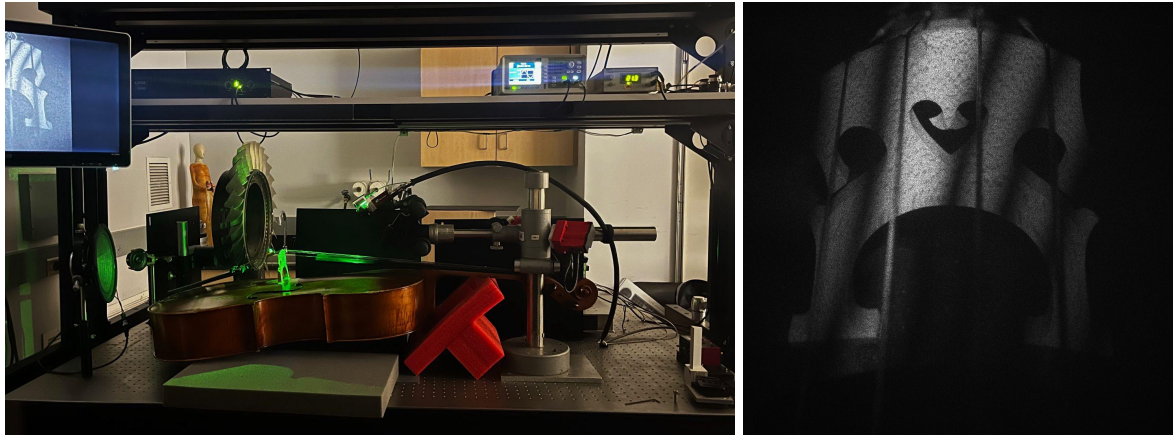
$$x(t) = \sin(t) + B' * (2t) + C' * \sin(3t) \quad (2.6)$$

Then string position can be shown graphically at time t through Eqs 2.5 and 2.6.

Sweeping through values of B and C at time 0 will give a maximum and minimum position of the first antinode of the string. This position can be used as a ratio over 2π for the antinode position of string with length L.

2.3 Time-Averaged Holographic Interferometry

Since the addition of a tuned mass damper directly affects cello bridge resonance, time-averaged holographic interferometry is used to identify resonant frequencies of the bridge before and after damper placement. After obtaining a preliminary list of frequencies from our SLDV, time-averaged holographic interferometry is used to focus on the bridge. The interferometry set-up involves laying the cello on its back on foam pads, with the speaker excitation source pointed at the underside of the bridge. The interferometer is mounted above and forward of the bridge, shining down onto the top panel. The first batch of images is taken from each major resonance frequency between 100 and 200 Hz. The speaker played a pure tone and the frequencies that produce notable fringes are captured. The bridge resonant frequencies do not match the body frequencies exactly, so the pure tone frequency is stepped up or down in increments of 1 Hz to locate exact resonant frequencies.



Figs 2.3 and 2.4: The experimental test setup used for holographic interferometry; a resultant signal image generated by the interferometer

After detecting and recording resonant frequency data, the results need to be processed. For this, MATLAB code was provided to us by Danny Ruiz-Cadalso of the CHSLT. The code uses the Goldstein 2d phase-unwrapping method for signal processing. The program takes .rti files generated by LaserView, masks out only the parts of the image to be analyzed, sets a “zero” point for the unwrapping algorithm, and then generates a displacement graph.

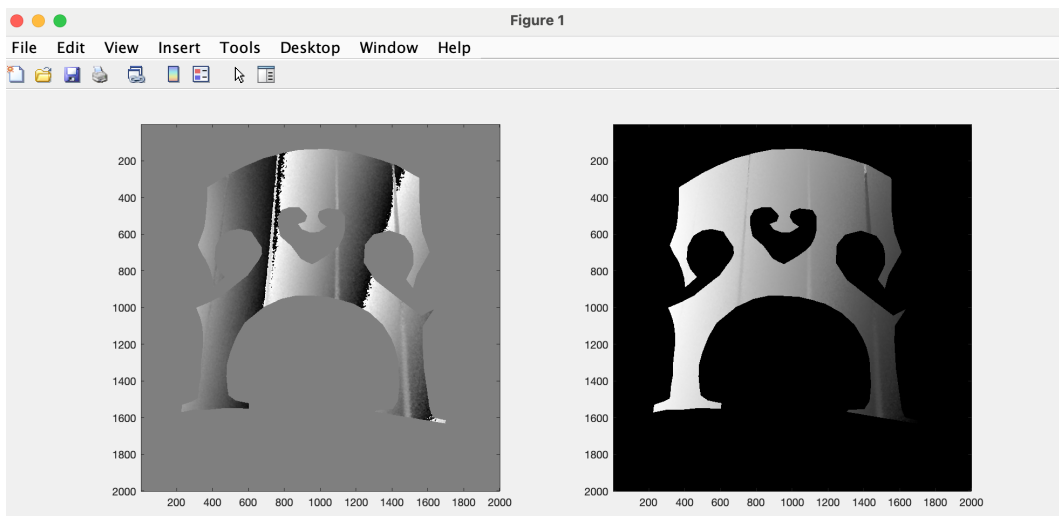
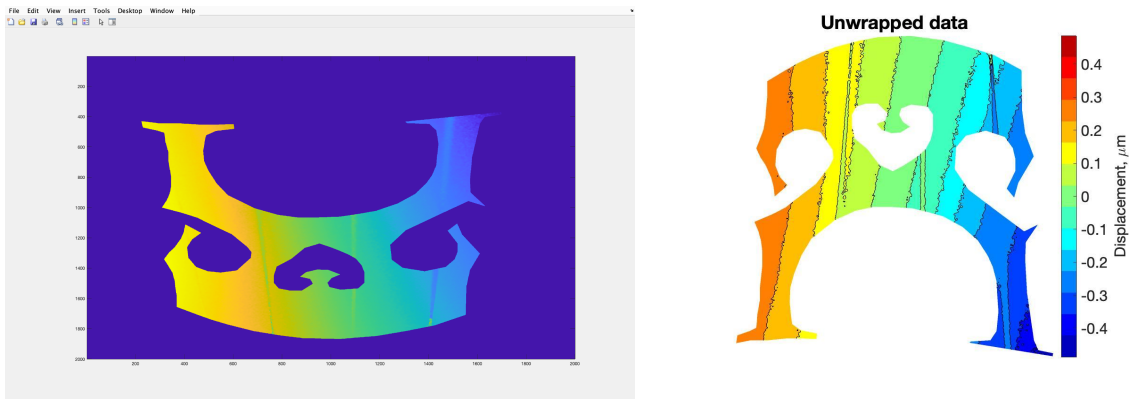


Fig 2.5: MATLAB window displaying the raw unwrapped data (left) and the filtered data (right)



Figs 2.6 and 2.7: The MATLAB interface to pick a “zero” point for the unwrapping algorithm; the generated displacement map upon conclusion of the program

2.4 Rerun Measurements

After placing the tuned mass damper, both scanning LDV and holographic interferometry measurements need to be run again with the same configurations. Comparison of results before and after placement gives a clear indication of damper effects. Since the damper acts on the string, scanning LDV results should remain unchanged at all frequencies between 0 and 400 Hz. However, resonant frequencies of the bridge should either disappear or move away from the measured cello body resonant frequency after placing the damper.

3. Results and Discussion

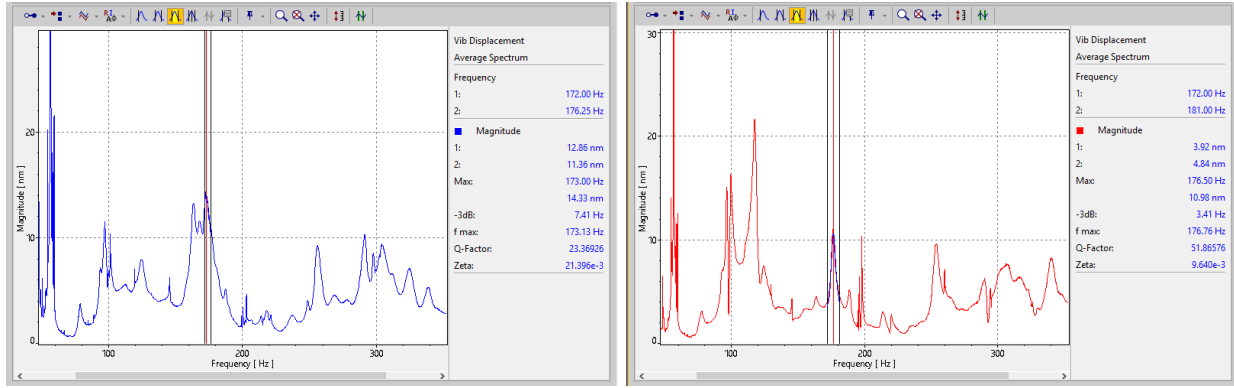
3.1 SLDV Results

Both SLDV scans used the same parameters: FFT, 3 levels of complex averaging, chirp between 0 and 400 Hz, 1600 frequency divisions, 1V speaker amplification, and a maximum velocity detection threshold of 5mm/s. The first scan, with the damper not present, identified six resonant modes within the scanning range. There was a seventh, very prominent resonant mode around 60 Hz, but it was considered out of the range of relevance to the wolf tone, and was

disregarded. Notably, there was a collection of three local maxima close to the wolf frequency, with resonance modes at 163.75, 168.25, and 173.00 Hz. After the optimal damper location was calculated, the SLDV scan was run again with the damper applied. The frequency-domain locations of the major resonance modes did not change with the application of the damper, with one major exception. However, the new resonance mode at 117.25 Hz was determined to be a result of different point placement causing some scanned points to fall on the string and damper. Also, the magnitude of the resonances was substantially different between runs. In the undamped test, the three strongest resonances were around 173 Hz, but with the damper applied, those resonance peaks were the weakest.

Undamped	Damped
97.75	96.5
—	117.25
163.75	164.00
168.25	171.25
173.00	176.75
256.25	254.00
291.50	290.00

Table 3.1: Resonance frequencies of the cello front body, generated using SLDV



Figs 3.1 and 3.2: Magnitude [nm] vs Frequency [Hz] spectrum of the cello front plate without damper applied (left) and with damper applied (right)

3.2 Damper Placement

Using critical frequency 173 Hz and first harmonic frequency 98 Hz, a plot of string vibration showed maximum displacements at x positions between 0.86337 and 1.10215 of a total length 2π . Therefore, the position of the damper was taken using the average at $0.98276/2\pi$ times the length of the string between the bridge and tailpiece. This length was recorded to be 6 inches, therefore, the tuned mass damper was placed 0.938 inches below the bridge. This coincides with previous research done on wolf dampers at low wolf tone frequencies shown in Figure 3.3. Green represents no wolf tone found after damper placement while red indicates wolf tone was easily found again after damper placement [2].

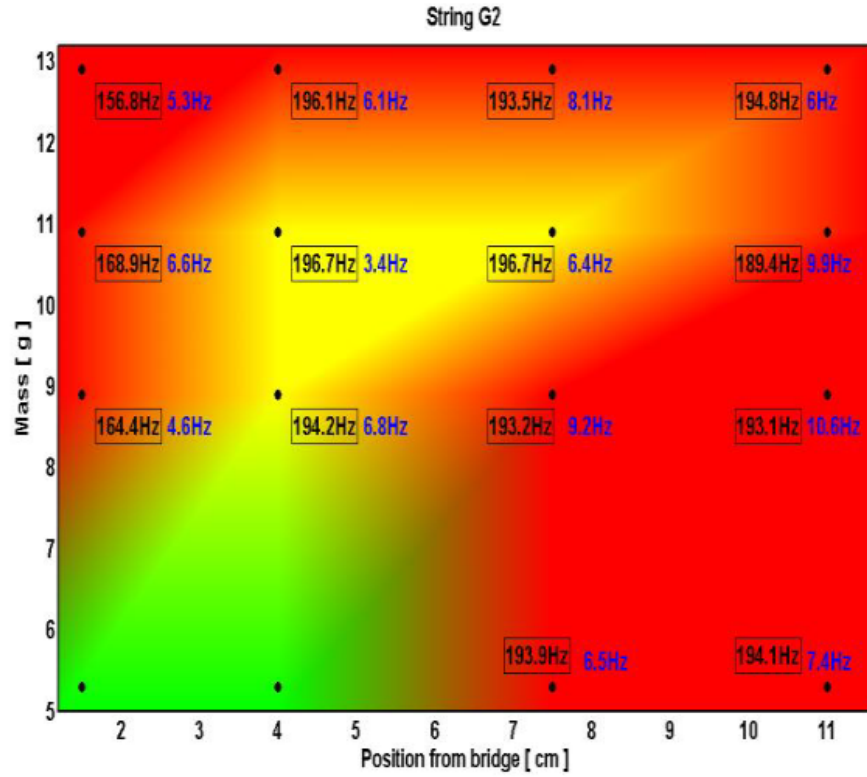


Fig. 3.3: Damper mass and position from bridge plotted as a function of ability to reproduce the wolf tone after placing the damper [3]

3.3 TAH1 Results

The holographic interferometry testing identified four resonance frequencies of the bridge between 100 and 200 Hz with the damper removed, and only three with the damper applied. Each of the undamped resonance frequencies was shared with the damped bridge, with the exact frequencies only shifting a few Hz at the absolute maximum. The resonance frequency of the bridge at 170 Hz dissipated entirely when the damper was applied.

Undamped	Damped
112	119
145	145
170	—
185	186

Table 3.2: Resonance frequencies of the cello bridge, generated using holographic interferometry

4. Conclusions and Recommendations

The overarching goals of the project were as follows: characterize the behavior of the cello around the frequency where wolf tone appears, calculate the location where the wolf damper is supposed to be applied, and verify that placing the wolf damper in the calculated location changes the resonant properties of the instrument around said frequency. We accomplished all of these goals, observing that the calculated location for damper placement was successful in reducing the wolf tone.

We used scanning LDV to observe the resonant responses of the cello front body as it was excited by an audio signal. This returned a fast fourier transform with the greatest magnitude concentrated around 170 Hz. This confirmed that the wolf tone, caused by playing a note with a frequency of about 170 Hz, is incited by a body resonance mode at the same frequency.

After the first SLDV scan was conducted, the optimal wolf damper location on the string between the bridge and tailpiece was calculated and matched results of another study. After applying the damper, we observed that playing the note had removed the presence of the wolf tone. The second SLDV scan returned similar resonant frequency values to the first, but with differing magnitudes. However, this can be explained by a different set of frequency points

between scans where the second scan had more points that overlapped with strings and the damper.

The bridge was then analyzed using TAHI, using the resonant frequency values that were located with the LDV scans. We identified four resonance frequencies of the bridge between 100 and 200 Hz with the damper off, with the most prominent one occurring at 170 Hz. TAHI was then redone with the damper applied, and the locations of the other resonance modes only changed slightly. The resonance mode at 170 Hz was entirely not present with the damper applied. This suggests that the counterweight of the wolf damper is successfully neutralizing the wolf tone.

Though the project accomplished its original goals, there is a substantial amount of further research to be done on the subject of bowed string instrument acoustical properties. More holography viewing the bridge from the top rather than the flat face could detect out-of-plane motion in the direction of the cello body. Since the bridge translates horizontal string vibration to vertical body movement, both top and front facing views would provide important information on bridge characteristics. Additionally, a Fourier spectrogram can be used to analyze the waveform and overtones of the wolf tone. Recording the auditory components of the tone with varying sizes, weights, and positions of the damper would be able to characterize quantitatively the effect of exact positioning in counteracting the wolf tone.

References

- [1] Brown, Gordon C., Pryputniewicz, Ryszard J. (1998). Holographic microscope for measuring displacement of vibrating microbeams using time-averaged, electro-optic holography. *Optical Engineering*, 37 (5): 1398–1405.
- [2] C. V. Raman (1916). “On the "Wolf note" of the violin and 'cello”. *Nature*, 97 (2435): 362–363. <https://doi.org/10.1038/097362a0>
- [3] V. Debut, O. Inacio, T. Dumas, J. Antunes (2010) *Modelling and experiments on string/body coupling and the effectiveness of a cello wolf-killing device*, International Symposium on Music Acoustics, Sydney, Australia.
- [4] Zhang, A., J. Woodhouse, G. Stoppani (2016). “Motion of the cello bridge”. *J. Acoust. Soc. Am*, 140 (4): 2636–2645. <https://doi.org/10.1121/1.4964609>